Measurement of Isolated Direct Photons in Lead-Lead Collisions at $\sqrt{s_{NN}} = 2.76$ TeV with the ATLAS Detector

Iwona Grabowska-Bold (for the ATLAS Collaboration)[1]

AGH University of Science and Technology, Al. A. Mickiewicza 30, Kraków, Poland

Abstract

Direct photons are a powerful tool to study heavy ion collisions. Their production rates provide access to the parton distribution functions, which are expected to be modified by nuclear effects. They also provide a mean to calibrate the energy of jets that are produced in the medium, and thus are a tool to probe the physics of jet quenching more precisely both through jet rates and fragmentation properties. The ATLAS detector measures photons with its hermetic, longitudinally segmented calorimeter, which gives excellent spatial and energy resolution, and detailed information about the shower shape of each measured photon. This gives powerful rejection against backgrounds from neutral pions produced in jets. Rejection against jet fragmentation products is further enhanced by isolation criteria, which can be based on energy flow in the calorimeter. First results on the rates of isolated direct photons from approximately 0.13 nb^{-1} of lead-lead data will be shown, as a function of transverse momentum, pseudorapidity and centrality.

1. Introduction

While jet quenching in heavy ion (HI) collisions at the Large Hadron Collider (LHC) was demonstrated using di-jet asymmetry distributions [1], the detailed physics mechanism of this phenomenon needs further understanding. One of the necessary factors in understanding jet quenching is having a proper calibration of the initial jet energy. Di-jet measurements are biased because it is not known whether or not the highest p_T jet was itself quenched. On the other hand single jet measurements [2, 3] at a given measured transverse momentum integrate over a range of initial unquenched jet energies. Therefore, another class of measurements which replaces one of the jets with an electroweak boson (γ, W or Z), opens the possibility of calibrating the energy of the accompanying jet [4]. The ATLAS and CMS collaborations have reported on the first correlation measurements of electroweak bosons with jets in Ref. [5, 6, 7].

As an important prerequisite of photon-jet measurements, it is essential to measure photon rates in lead-lead collisions. At high energy prompt photons are expected to have two primary sources; the first is direct emission, which proceeds via quark-gluon Compton scattering $qg \to q\gamma$ or quark-antiquark annihilation $q\bar{q} \to g\gamma$, the second is the production of a single hard photon during parton fragmentation, called fragmentation contribution.

[1] A list of members of the ATLAS Collaboration and acknowledgements can be found at the end of this issue.

In this proceedings, a measurement of isolated prompt photons in lead-lead collisions at $\sqrt{s_{NN}}$ = 2.76 TeV with the ATLAS detector [8] is presented and discussed. Yields per event are measured averaged over $|\eta| < 1.3$ and as a function of event centrality and photon transverse momentum p_T ranging from 45 to 200 GeV.

2. Event Selection

The sample of events used in this analysis was collected in the 2011 HI run using the first level electromagnetic calorimeter trigger [9], which requires a cluster of cells with transverse energy exceeding E_T = 16 GeV. This trigger is found to be 100% efficient for photons with $E_T > 20$ GeV. Analyzed events are divided into centrality classes, which are defined based on a total sum of E_T in the forward calorimeter [10].

Photons are reconstructed using information from the ATLAS calorimeter after underlying event (UE) background subtraction. A sliding window algorithm is seeded on the second layer of the electromagnetic calorimeter, which typically samples over 50% of the deposited photon energy. The energy measurement is made using all three layers of the electromagnetic calorimeter and the presampler. The photon conversion recovery procedure is not performed, due to the overwhelming number of combinatorial pairs in more central collisions in the high track multiplicity environment of the HI collision. Therefore, a substantial fraction of converted photons is still reconstructed by the photon algorithm. Following the reconstruction requirements, further photon identification cuts are made. The fine-grained, longitudinally segmented calorimeter allows detailed characterization of the shape of each photon shower, providing tools to reject jets and hadrons, while maintaining the high efficiency for the photons themselves. Nine shower shape variables are used in this analysis [11]. Along with the kinematic cuts they constitute the photon selection. After application of the photon cuts to the 0-80% centrality class, but before applying isolation requirements, there are 6435 photon candidates.

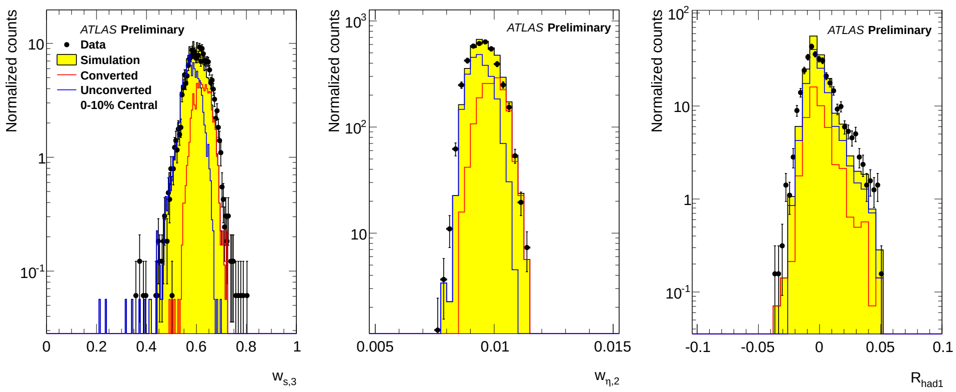

Figure 1: Comparisons of three photon identification variables for data (black points) with results from simulation for 0-10% central events [11]. $w_{s,3}$ is the RMS width of the three cells including and surrounding the cluster maximum in the first calorimeter layer. $w_{\eta,2}$ is the RMS width of the energy distribution of the cluster in the second layer in the η direction and R_{had1} is the ratio of transverse energy measured in the first layer of the hadronic calorimeter to the transverse energy of the photon cluster. Error bars represent statistical uncertainties. The simulation is shown both fully integrated (yellow) and broken out into contributions from unconverted photons (red histogram) and converted photons (blue histogram).

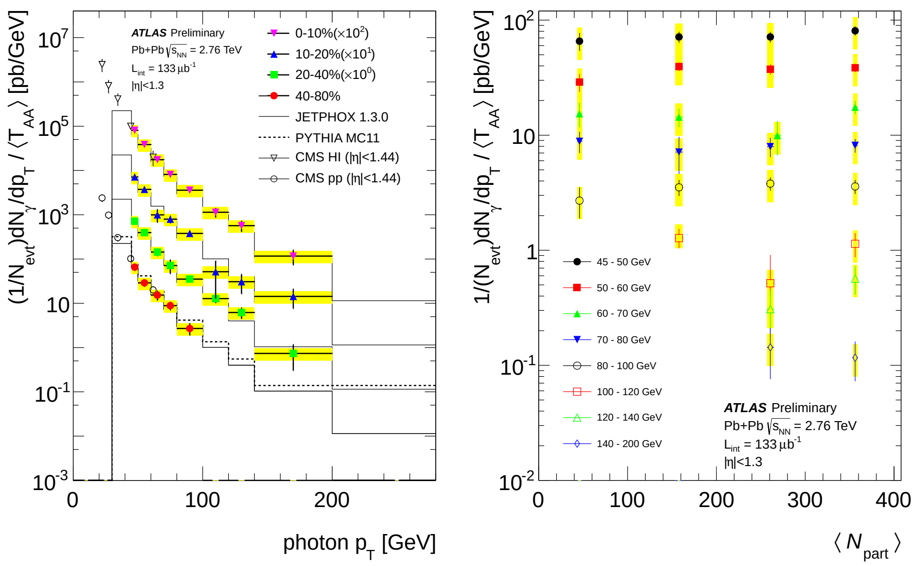

Figure 2: (left) Efficiency corrected yields of prompt photons in $|\eta| < 1.3$ using photon cuts, isolation cone radius $R_{iso} = 0.3$ and isolation transverse energy of 6 GeV. (right) Centrality dependence of the photon yield per event in each p_T bin, scaled by the average nuclear thickness function $\langle T_{AA}\rangle$ for that centrality interval. The horizontal axis is the average number of participants $\langle N_{part}\rangle$ for each selected centrality interval. Statistical errors are shown by the error bars. Systematic uncertainties on the photon yields are combined and shown by the yellow bands [11].

Figure 1 shows three shower shape variables for data from the 0-10% centrality bin, compared to the Monte Carlo (MC) simulation. In all cases, electromagnetic clusters with reconstructed transverse energy greater than 40 GeV and $|\eta| < 1.3$ are shown. The simulation also allows to inspect the contributions from converted and unconverted photons. It is found that the broad features of the distributions are reproduced well by the simulation.

In order to reduce the contribution of di-jet background events, as well as events containing fragmentation photons, an isolation criterion is applied within a cone aligned with the photon direction. The isolation transverse energy, $E_T(R_{iso})$, defined as the sum of transverse energies in the calorimeter cells in a cone $\sqrt{\Delta\eta^2 + \Delta\phi^2} < R_{iso} = 0.3$ around the photon axis after the UE background subtraction, is required to be less than 6 GeV.

3. Results

The double sideband technique [11] is applied to extract the photon yield per minimum bias event $(1/N_{evt})dN_\gamma/dp_T(p_T, c)$, divided by the mean nuclear thickness $\langle T_{AA}\rangle = \langle N_{coll}\rangle/\sigma_{tot}^{pp}$ which scales as the number of binary collisions $\langle N_{coll}\rangle$, where σ_{tot}^{pp} is the total inelastic pp cross section. The photon yield is defined as:

$$\frac{1}{N_{evt}}\frac{dN_\gamma}{dp_T}(p_T, c) = \frac{N^{sig}}{\epsilon_{tot} \times N_{evt} \times \Delta p_T},$$

where N^{sig} is the background-subtracted yield of direct photons, ϵ_{tot} is the total photon reconstruction efficiency defined as the probability that a photon would be reconstructed, identified and isolated, N_{evt} is the number of events recorded with a minimum bias trigger [12] in the centrality bin c and Δp_T is the width of the transverse momentum interval. The photon yields divided by $\langle T_{AA} \rangle$ are shown in the left panel of Figure 2 for different bins of centrality. The results are scaled in centrality intervals, except for the 40-80% bin, as labeled in the figure for visibility reasons. The systematic uncertainties are indicated by yellow bands with the biggest contributions from the photon selection cuts and the isolation criterion at the level of 20% each. Also CMS data [13] for 0-10% central HI collisions and $|\eta| < 1.44$, which is a 10% larger interval in η comparing to ATLAS, and a tighter isolation condition $E_T(R_{iso} = 0.4) < 5$ GeV are superimposed on the most central bin. CMS pp data [13] from $\sqrt{s} = 2.76$ TeV, superimposed on the most peripheral bin, are also shown. The two sets of measurements agree in shape and normalization.

The right panel of Figure 2 shows the photon yield divided by $\langle T_{AA} \rangle$ in each p_T interval as a function of the number of participants $\langle N_{part} \rangle$. It can be seen that there is no significant centrality dependence in any of the measured p_T intervals. This indicates that photon production rates in HI collisions scale linearly with the mean nuclear thickness, or equivalently with the average number of binary collisions.

4. Summary

In this proceedings, measurements of isolated prompt photon yields in lead-lead collisions are shown as a function of collision centrality in a kinematic range of $45 < p_T < 200$ GeV and $|\eta| < 1.3$. Photons have been reconstructed using the large-acceptance, longitudinally fine segmented ATLAS electromagnetic calorimeter, after event-by-event subtraction of the underlying event background. After scaling the yields by the mean nuclear thickness $\langle T_{AA} \rangle$, photon production rates are observed to be constant as a function of centrality within experimental uncertainties. This observation implies a linear scaling with the number of binary collisions indicating that photons are a useful tool for calibrating the initial momentum transfer of the hard process, which will be important for future jet quenching measurements.

References

[1] ATLAS Collaboration, Phys. Rev. Lett. 105, 252303 (2010).

[2] ATLAS Collaboration, J. Phys. G 38, 124021 (2011).

[3] ATLAS Collaboration, J. Phys. G 38, 124085 (2011).

[4] X. -N. Wang, Z. Huang and I. Sarcevic, Phys. Rev. Lett. 77, 231 (1996).

[5] ATLAS Collaboration, "Measurement of the correlation of jets with high p_T isolated prompt photons in lead-lead collisions at $\sqrt{s_{NN}} = 2.76$ TeV with the ATLAS detector at the LHC", ATLAS-CONF-2012-121, https://cdsweb.cern.ch/record/1473135.

[6] ATLAS Collaboration, "Measurement of momentum imbalance in $Z \rightarrow ll$ + jet events in Lead-Lead collisions at $\sqrt{s_{NN}} = 2.76$ TeV with the ATLAS detector", ATLAS-CONF-2012-119, https://cdsweb.cern.ch/record/1472941.

[7] CMS Collaboration, "Studies of jet quenching using isolated-photon+jet correlations in PbPb and pp collisions at $\sqrt{s_{NN}} = 2.76$ TeV", CMS-HIN-11-010, http://arxiv.org/abs/1205.0206.

[8] ATLAS Collaboration, JINST 3, S08003 (2008).

[9] ATLAS Collaboration, Eur. Phys. J. C72 1849 (2012).

[10] ATLAS Collaboration, Phys.Lett. B710 363-382 (2012).

[11] ATLAS Collaboration, "Measurement of high-p_T isolated prompt photons in lead-lead collisions at $\sqrt{s_{NN}} = 2.76$ TeV with the ATLAS detector at the LHC", ATLAS-CONF-2012-051, https://cdsweb.cern.ch/record/1451913.

[12] ATLAS Collaboration, "Performance of the ATLAS Minimum Bias and Forward Detector Triggers in 2011 Heavy Ion Run", ATLAS-CONF-2012-122, https://cdsweb.cern.ch/record/1473425.

[13] CMS Collaboration, Phys. Lett. B 710, 256 (2012).